Kinetic Model for Noncatalytic Supercritical Water Gasification of Cellulose and Lignin

Fernando L. P. Resende and Phillip E. Savage
Dept. of Chemical Engineering, University of Michigan, 2300 Hayward, St. Ann Arbor, MI, 48109

DOI 10.1002/aic.12165
Published online January 22, 2010 in Wiley Online Library (wileyonlinelibrary.com).

This article reports the first kinetics model for Supercritical Water Gasification (SCWG) that describes the formation and interconversion of individual gaseous species. The model comprises 11 reactions, and it uses a lumping scheme to handle the large number of intermediate compounds. We determined numerical values for the rate constants in the model by fitting it to experimental data previously reported for SCWG of cellulose and lignin. We validated the model by showing that it accurately predicts gas yields at biomass loadings and water densities not used in the parameter estimation. Sensitivity analysis and reaction rate analysis indicate that steam-reforming and water–gas shift are the main sources of H_2 in SCWG, and intermediate species are the main sources of CO, CO_2, and CH_4. © 2010 American Institute of Chemical Engineers *AIChE J,* 56: 2412–2420, 2010

Keywords: cellulose, lignin, gasification, supercritical water, kinetic model

Introduction

Developing methods to use the chemical energy in biomass more readily is one pathway to a more sustainable energy supply. Attractive features of biomass are that it is a renewable resource available in large amounts in many areas of the world, the eventual oxidation of its carbon atoms does not increase the net amount of CO_2 in the atmosphere, and many biomass feedstocks are wastes that would be eliminated in the process of converting them to fuels.

Gasification is one approach for biomass utilization. In conventional gasification, biomass is converted into H_2, CH_4, CO, CO_2, char, and tar.[1–3] The char and tar represent a loss of useful carbon, and the tar can be difficult to separate from the product gas stream.[4,5] Another drawback in conventional biomass gasification is the energy required to dry biomass feedstocks, which very often have more than 50% moisture.[6] The thermal efficiency of conventional gasification drastically decreases as the biomass moisture content increases.[7]

Supercritical Water Gasification (SCWG) has been proposed as an alternative approach that avoids these difficulties. In this process, water above its critical point (374°C and 22 MPa) is the medium for gasification reactions. The presence of supercritical water (SCW) fundamentally changes the gasification process. SCW can dissolve cellulose and lignin, the main components of woody biomass, and thereby create a homogeneous medium in which hydrolysis reactions dominate.[4,8–10] As a result, the amount of by-products (such as char and tar) is minimized, leading to higher gas yields.[8,11–14]

Rate laws and kinetic parameters are essential for the design of reactors and estimation of product distribution. The few previous kinetic models[8,15–18] for SCWG focus solely on gasification yields or feedstock conversion, without capturing the pathways leading to formation and interconversion of gas species. There are no published kinetic models dealing with individual gas yields for SCWG. As a result, little is known about the rates of different potential reaction paths. For instance, the methanation reaction takes place under SCWG conditions, but it is not known whether most of the CH_4 formed actually originates from methanation or possibly from other gasification routes, such as direct pyrolytic cleavage of methyl groups present in lignin. If most of the CH_4 originates from methanation, how close to equilibrium is this reaction at typical SCWG conditions? Could catalysts be used to increase CH_4 yields? These are some of the questions one could begin to answer with the aid of a reliable kinetic model that includes information about yields of individual gaseous products.

Correspondence concerning this article should be addressed to P. E. Savage at psavage@umich.edu.

We developed a kinetic model for noncatalytic SCWG of commercially available microcrystalline cellulose and organosolv lignin and fit it to experimental data obtained in quartz reactors.[19] By using quartz, we avoided unintentional catalytic contributions from metallic reactor walls. One objective of this modeling work is to identify the reaction pathways leading to the formation of specific gases and to quantify rates of formation. The first part of this article describes the reaction pathways in the model. The second part describes the parameter estimation procedure, results, and comparisons of model predictions with experimental measurements. In the final part, we use the model to identify the reactions that are most important for forming the different gases.

Model Development

The model is based on reaction pathways proposed in the literature for SCWG. It focuses on reactions involving gas species and simplifies reactions involving larger intermediate compounds by defining a generic intermediate species into which all actual intermediates are lumped. Following, we define the reactions involved in the model.

Reaction 1. Hydrolysis

$$\text{For Cellulose :} \quad (C_6H_{10}O_5)_n + n\,H_2O \xrightarrow{k_1} n\,C_6H_{12}O_6$$

$$\text{For Lignin :} \quad (C_{10}H_{10}O_3)_n + n\,H_2O \xrightarrow{k_1} n\,C_{10}H_{12}O_4$$

When cellulose (or lignin) is in water at supercritical conditions, the first step[1] is solvation of the biomacromolecules. This physical process takes place simultaneously with hydrolytic attack on the macromolecular structures. This very fast step often leads to the formation of oligomers, such as cellobiose and cellotriose originating from cellulose. These oligomers can be further hydrolyzed. For the purpose of this model, we assume that hydrolysis leads directly and solely to monomers. The monomer for cellulose is glucose, and the monomer for lignin is based on the elemental composition of organosolv lignin.[20] Sasaki et al.[21] showed that cellulose is completely converted in water at 350°C and 25 MPa after only 4 s. Bobleter[22] reported that over 90% of lignin disappears after only 0.4 min at 365°C. Given this literature data, we take the initial reactant to be the monomer instead of the biopolymer itself.

Reaction 2. Intermediate Formation.

$$\text{Monomer} \xrightarrow{k_2} C_xH_yO_z$$

Once the monomer is formed, it can undergo a variety of reactions leading to numerous decomposition products. Glucose, for instance, can undergo isomerization, dehydration, retro-aldol condensation, and hydrolysis.[4,13] A key concept in this model is the treatment of all the different intermediate compounds as a single pseudo-component. Rather than monitoring and explicitly accounting for every possible intermediate compound, we adopted this lumping scheme for the intermediates. We define the intermediate species as $C_xH_yO_z$, which represents any nonpermanent gas originating from the biomass that is capable of reacting further. These intermediates ultimately lead to the formation of gases.

Reactions 3 and 4. Steam-Reforming.

Steam-Reforming I

$$C_xH_yO_z + (x - z)H_2O \xrightarrow{k_3} x\,CO + (x - z + y/2)H_2$$

Steam-Reforming II

$$C_xH_yO_z + (2x - z)H_2O \xrightarrow{k_4} x\,CO_2 + (2x - z + y/2)H_2$$

One of the ways organic compounds form gases in the presence of water is via steam-reforming. The intermediate $C_xH_yO_z$ reacting with water leads to CO and H_2 (Steam-reforming I), or CO_2 and H_2 (Steam-Reforming II). To handle the stoichiometry in the steam reforming calculations in the model, we take the intermediate species to have the same chemical composition as the original monomer.

Reactions 5 to 8. Intermediate Decomposition.

$$\text{CO from Intermediate} \quad C_xH_yO_z \xrightarrow{k_5} CO + C_xH_yO_z$$

$$\text{CO}_2\text{ from intermediate} \quad C_xH_yO_z \xrightarrow{k_6} CO_2 + C_xH_yO_z$$

$$\text{CH}_4\text{ from intermediate} \quad C_xH_yO_z \xrightarrow{k_7} CH_4 + C_xH_yO_z$$

$$\text{H}_2\text{ from intermediate} \quad C_xH_yO_z \xrightarrow{k_8} H_2 + C_xH_yO_z$$

Our experimental results[19] suggest that steam-reforming alone cannot accurately describe the way gases are formed in noncatalytic SCWG. There are multiple ways the intermediates can decompose to form gases. For instance, in the case of lignin decomposition, methyl groups in the intermediates can be cleaved thermally, directly leading to the formation of CH_4. To account for these pathways, we introduced the possibility of direct formation of the gas species from the lumped intermediates. Also, each intermediate molecule can undergo decomposition reactions multiple times, releasing small molecules such as H_2 or CO and creating a new intermediate molecule each time. Since all intermediates are lumped together, however, there is no net consumption of intermediates in these steps.

Reaction 9. Char Generation.

$$C_xH_yO_z \xrightarrow{k_9} \text{Char}$$

Intermediate species in SCWG can react to form compounds that eventually become char. In our model, we lump all such compounds together and refer to them collectively as char. We assume that these molecules do not react to form gases.

Reactions 10 and 11. Gas species interconversion.

$$\text{Water–Gas Shift} \quad CO + H_2O \leftrightarrow CO_2 + H_2$$

$$\text{Methanation} \quad CO + 3\,H_2 \leftrightarrow CH_4 + H_2O$$

Once the gas species are formed, reactions 10 and 11 can change their relative amounts. The water–gas shift reaction consumes CO and is thought to be one of the main reaction pathways for the production of H_2. Likewise, methanation is often invoked as an important route for the formation of CH_4. Water–gas shift and methanation are the only reversible reactions in this model. We considered the possibility of adding other typical gasification reactions such as hydrogenation and

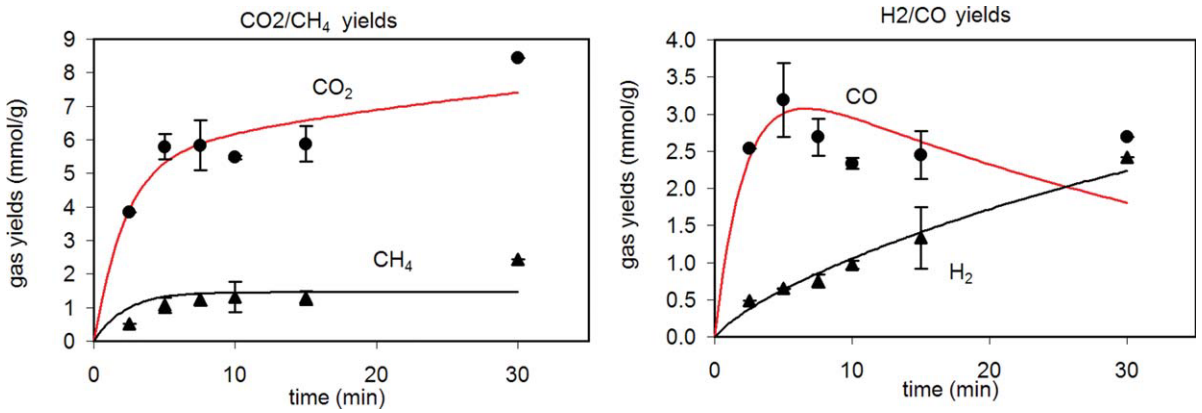

Figure 1. Base case fitting for cellulose SCWG (500°C, 0.08 g/ml, 9.0 wt %).

[Color figure can be viewed in the online issue, which is available at wileyonlinelibrary.com.]

the Boudouard reaction, but equilibrium calculations done in ASPEN Plus showed that these reactions do not take place to any appreciable extent at the conditions of this work (500–600°C). These calculations are described elsewhere.[23]

The rate equation for each reaction was assumed to be first order in the concentration (C) of each species in the reaction. We used isothermal constant-volume quartz batch reactors for all experiments, so the reaction engineering analysis is straightforward. Following are the mole balance equations for each of the species.

$$\frac{dC_{CO_2}}{dt} = xk_4C_IC_W + k_6C_I + k_{10}C_{CO}C_W - k_{10r}C_{CO_2}C_{H_2} \quad (1)$$

$$\frac{dC_{CO}}{dt} = xk_3C_IC_W + k_5C_I - k_{10}C_{CO}C_W + k_{10r}C_{CO_2}C_{H_2} - k_{11}C_{CO}C_{H_2} + k_{11r}C_{CH_4}C_W \quad (2)$$

$$\frac{dC_{CH_4}}{dt} = k_7C_I + k_{11}C_{CO}C_{H_2} - k_{1lir}C_{CH_4}C_W \quad (3)$$

$$\frac{dC_{H_2}}{dt} = (x - y + y/2)k_3C_IC_W + (2x - z + y/2)k_4C_IC_w + k_8C_I + k_{10}C_{CO}C_W - k_{10r}C_{CO_2}C_{H_2} - 3k_{11}C_{CO}C_{H_2} + 3k_{11r}C_{CH_4}C_W \quad (4)$$

$$\frac{dC_I}{dt} = k_2C_M - k_3C_IC_W - k_4C_IC_W - k_9C_I \quad (5)$$

$$\frac{dC_M}{dt} = -k_2C_M \quad (6)$$

$$\frac{dC_W}{dt} = -(2x - z)k_4C_IC_W - k_{10}C_{CO}C_W + k_{10r}C_{CO_2}C_{H_2} + k_{11}C_{CO}C_{H_2} - k_{11r}C_{CH_4}C_W \quad (7)$$

The subscripts I, M, and W represent the lumped intermediate compounds, the lignin or cellulose monomer, and water, respectively.

Results and Discussion

This section provides results from the model parameter estimation and then assesses the predictive ability of the model. The final portions present results from the model being exercised to reveal the fastest reaction paths and the paths to which the model predictions are most sensitive.

Parameter estimation

The temporal variation of the experimental gas concentrations (CH_4, CO_2, CO, and H_2) at the "base case" conditions in our previous article[19] for cellulose and lignin were used to determine the model parameters. The base case conditions are 500°C (cellulose), 600°C (lignin), 0.08 g/ml water density, and 9.0 wt % biomass loading. We take the term biomass to include the lignin and cellulose fractions of interest in this article. Experiments were performed from 2.5 to 30 minutes for cellulose, and from 2.5 to 75 minutes for lignin. These data were obtained in a kinetically controlled region for SCWG as the system was far from equilibrium and likely free of any mass transfer limitations on the observed rates.

For the SCWG experiments,[19] the average particle size for cellulose was 116 μm, and for lignin it was 289 μm. Simmons and Gentry[24] showed that pyrolysis of cellulose in the range 450–500°C is free from mass transfer limitations for particles as large as 200 μm. Vamvuka et al.[25] performed TGA for several biomass feedstocks and measured kinetics without mass-transfer limitations using particles of 250 μm. On the basis of this literature, we believe that mass transfer limitations can be safely neglected in this study.

The objective function that was minimized is the unweighted sum of the squared differences between calculated and measured concentrations of the four gases. Scientist 3.0 from Micromath was used to fit the experimental data. Initial guesses for the rate constants were found manually by a trial-and-error method. Polymath 5.1 was used for the model simulations after the rate constants were determined.

The rate constants determined from the experimental SCWG data were k_2, k_3, k_4, k_5, k_6, k_7, k_8, k_9, k_{10}, and k_{11}. The rate constants for the reverse reactions (k_{10r} and k_{11r}) were related to the forward rate constants (k_{10} and k_{11}) by the equilibrium constant K:

$$k_r = \frac{k_f}{K} \quad (8)$$

The equilibrium constants for the water–gas shift and methanation reactions were calculated using output from the REQUIL reactor block in ASPEN Plus. This block provides

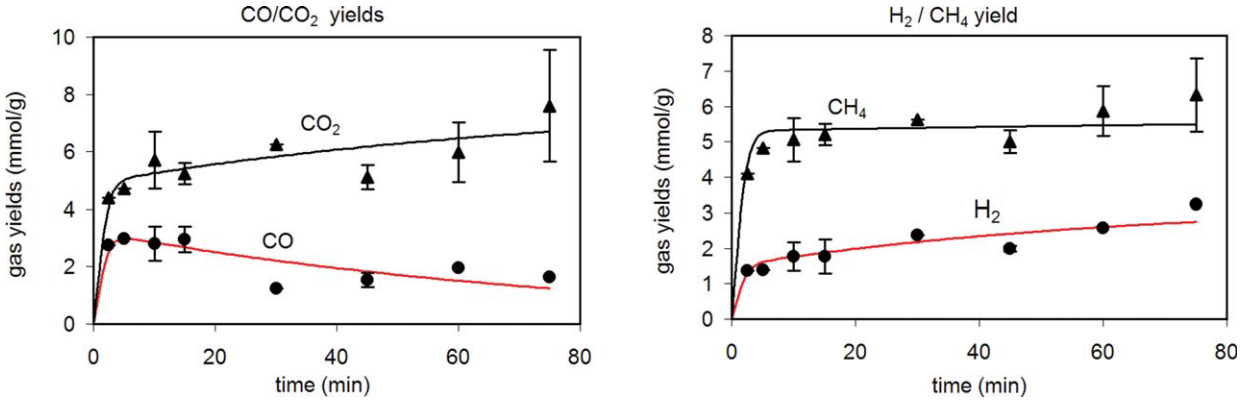

Figure 2. Base case fitting for lignin SCWG (600°C, 0.08 g/ml, 9.0 wt %).

[Color figure can be viewed in the online issue, which is available at wileyonlinelibrary.com.]

equilibrium concentrations for a given reaction, from which we calculated K_{10} (equilibrium constant for the water–gas shift) and K_{11} (equilibrium constant for methanation) using Eqs. 9 and 10:

$$K_{10} = \frac{C_{H_2}.C_{CO_2}}{C_{CO}.C_{H_2O}} \quad (9)$$

$$K_{11} = \frac{C_{CH_4}.C_{H_2O}}{C_{CO}.C_{H_2}^3} \quad (10)$$

For the water–gas shift reaction, the equilibrium constant was 5.15 at 500°C and 2.68 at 600°C. For methanation, the equilibrium constant was 3.62×10^5 l^2/mol^2 at 500°C and 1.02×10^4 l^2/mol^2 at 600°C. Additional details about these equilibrium constant calculations are available elsewhere.[23]

Figures 1 and 2 show the base case experimental results along with the model calculations for cellulose and lignin. Table 1 lists the rate constants. CO is rapidly formed in the initial minutes, reaches a maximum, and then is consumed at longer times. The CO_2 and CH_4 formation rates are also high in the initial minutes, but they become much lower at longer times. The yield of H_2 increases steadily for cellulose, whereas for lignin it increases more rapidly during the initial minutes. The model clearly captures the trends in the data and fits the temporal variation of the gas yields at the base case conditions very well for both cellulose and lignin.

Table 1. Rate Constants at 500°C (Cellulose) and 600°C (Lignin)

	Cellulose	Lignin
k_2 (min^{-1})	2.00×10^0	1.67×10^0
k_3 (min^{-1}) or (L mol^{-1} min^{-1})	1.16×10^{-3}	5.00×10^{-4}
k_4 (L mol^{-1} min^{-1})	0.00×10^0	2.73×10^{-3}
k_5 (min^{-1})	2.47×10^{-1}	5.39×10^{-1}
k_6 (min^{-1})	4.25×10^{-1}	7.67×10^{-1}
k_7 (min^{-1})	1.11×10^{-1}	9.42×10^{-1}
k_8 (min^{-1})	2.68×10^{-3}	0.00×10^0
k_9 (min^{-1})	4.65×10^{-1}	9.38×10^{-1}
k_{10} (L mol^{-1} min^{-1})	6.11×10^{-3}	2.80×10^{-3}
k_{10r} (L mol^{-1} min^{-1})	1.19×10^{-3}	1.05×10^{-3}
k_{11}(L mol^{-1} min^{-1})	0.00×10^0	7.71×10^{-2}
k_{11r} (L mol^{-1} min^{-1})	0.00×10^0	7.52×10^{-6}

In addition to adequately fitting the experimental data, one expects a kinetics model to use rate constants that have reasonable values. Of all the reactions in the model, only the water–gas shift reaction has been the subject of kinetics studies e.g.,[26–28] in supercritical water. Only the work of Rice et al.,[26] however, provides experimental kinetics data from studies that encompass a temperature (500°C) and the water density (0.08 g/cm^3) used to determine the model parameters. Rice et al.[26] measured the rate constant at 520 and 480°C for many different water concentrations (densities) and showed that the rate constant has a very strong density dependence. Using their data, we estimated rate constant values at 0.08 g/cm^3 for both 480 and 520°C. We then used these values and the Arrhenius equation to estimate the rate constant at 0.08 g/cm^3 and 500°C. The value we obtain is 1.5×10^{-3} L mol^{-1} min^{-1}, which is the same order of magnitude as the value we obtained by fitting the model to the cellulose gasification data at 500°C (see value for k_{10} in Table 1). We consider this level of agreement with the literature to be very good, given that the water–gas shift rate constants from different experimental studies at a given temperature varied by as much as two orders of magnitude.[28] We are aware of no kinetics studies of the water gas shift reaction at 600°C, so we cannot compare this value with previous experiments.

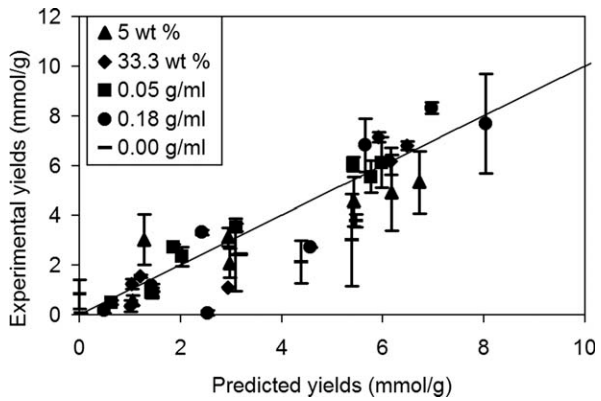

Figure 3. Model predictions for gas yields from cellulose (10 min for wt %, 7.5 min for g/ml) and lignin SCWG (75 min for wt %, 60 min for g/ml).

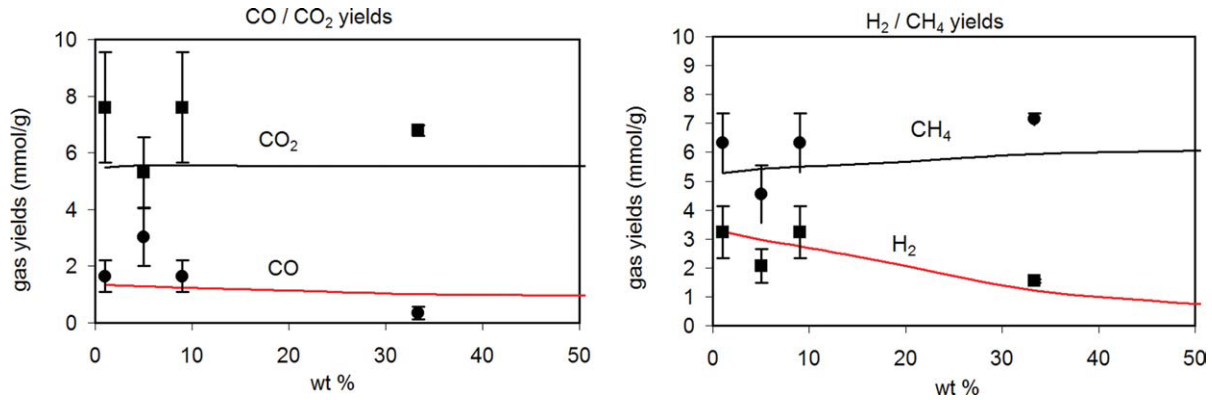

Figure 4. Effect of lignin loading (75 min).

[Color figure can be viewed in the online issue, which is available at wileyonlinelibrary.com.]

One expects rate constants to increase as the temperature increases, but the water–gas shift rate constants from the model in Table 1 do not meet this expectation. We believe that this behavior results from uncertainty in the rate constant estimates rather than from actual non-Arrhenius behavior for this reaction. Given that the precise values obtained for the water–gas shift kinetics in the model depend on the values of all other parameters (because of the covariance between parameters) it is likely that, if desired, a set of parameters could have been obtained that included an Arrhenius dependence for water–gas shift. We did not consider this feature to be a requirement since it was not central to the purposes of our modeling effort.

Model validation

Having demonstrated that the model can fit the base case data for cellulose and lignin, we next test its predictive capabilities. In this section we use the model to predict the results of SCWG experiments done at the base case temperatures but different water densities or biomass loadings. We also use the model to predict equilibrium compositions for SCWG.

We used the model to predict the gas yields from SCWG at the base case temperatures but at different biomass loadings (5.0 and 33.3 wt %) and different water densities (0.00 g/ml, 0.05 g/ml, 0.18 g/ml). Figure 3 is a parity plot that compares the experimental[19] and predicted yields. If the model predictions were perfect, all of the data would fall on the diagonal line shown. Figure 3 shows that the model can predict the results for most of the gas yields at the different biomass loadings for both cellulose and lignin with good proximity. The model seems to perform worst for the case of pyrolysis (0.00 water density). Even here, however, the model predictions often fell within the experimental uncertainty.

We next compare experimental results and model predictions regarding how the gas yields change with biomass loading and water density. For cellulose, the model predicts very little effect of the biomass loading on yields. This finding is in good agreement with experiments.[19] Since there was no effect, we do not compare these results in a separate graph. For lignin, the biomass loading has a larger effect on some gas yields, as shown in Figure 4. The model captures the slight decreases in the H_2 and CO yields as the lignin loading increases, as well as the slight increase in CH_4. The CO_2 yield appears to remain loading invariant.

The effect of water density on gas yields is shown for cellulose in Figure 5 and for lignin in Figure 6. The model identifies the main trends for cellulose and lignin, matching the experimental trends reasonably well in most cases. The CO yield decreases with water density, while the H_2 yield increases. The CO_2 yield slightly increases with water density, and the CH_4 yield remains nearly unchanged. The

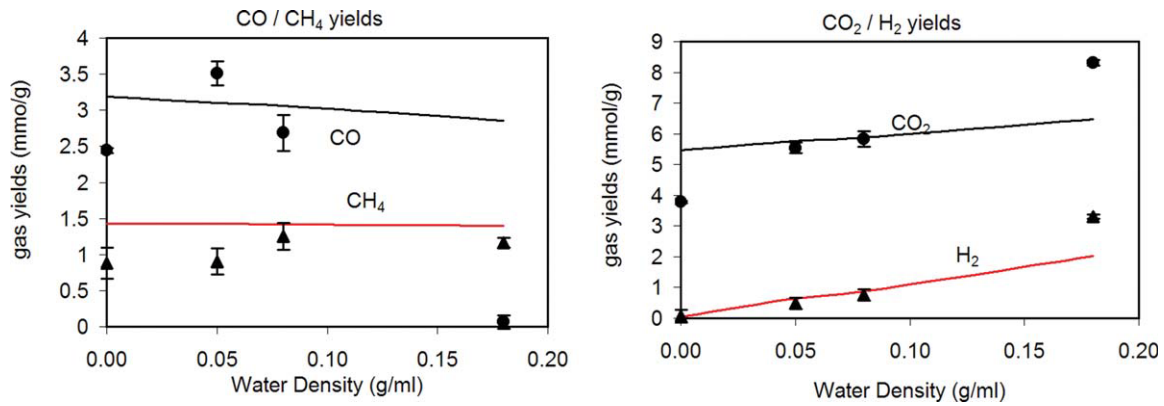

Figure 5. Effect of water density for cellulose (7.5 min).

[Color figure can be viewed in the online issue, which is available at wileyonlinelibrary.com.]

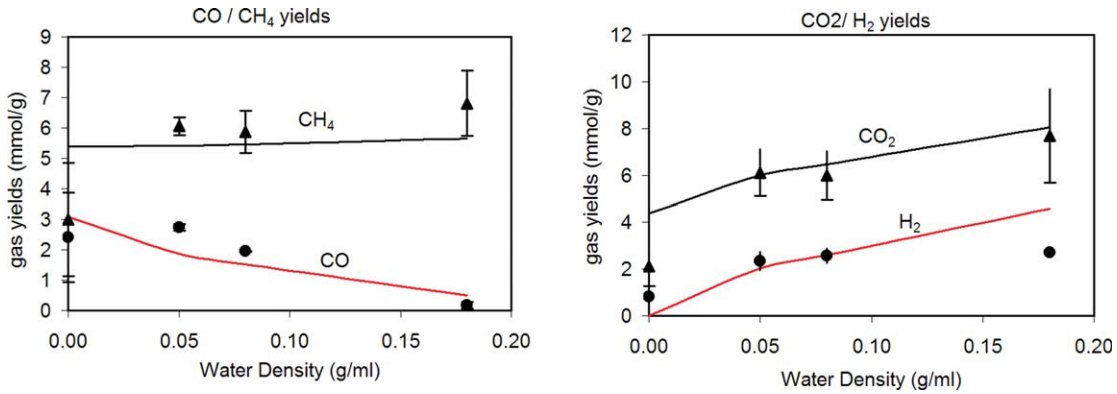

Figure 6. Effect of water density for lignin (60 min).

[Color figure can be viewed in the online issue, which is available at wileyonlinelibrary.com.]

largest differences between experimental data and model predictions are for pyrolysis and at the highest water density, 0.18 g/ml (especially for cellulose). These differences are possibly because of the documented[26,27] dependence of the water–gas shift kinetics on the water density. The model uses a rate constant for water–gas shift that is density independent.

Having tested the model by making predictions at different biomass loadings and water densities at different times, we now turn our attention to equilibrium. If the model includes the essential set of gas-phase reactions for SCWG, it should be able to predict the equilibrium product distributions. We simulated equilibrium SCWG by running the kinetics model to very long batch holding times (40,000 min for lignin), such that the yields became time invariant. That such a long reaction time was needed to reach equilibrium clearly indicates that the gaseous products were far from equilibrium at the much shorter reaction times investigated experimentally. Good catalysts for water–gas shift and methanation would be essential for reaching equilibrium more quickly.

We previously reported[19] equilibrium compositions for lignin SCWG at the base case conditions based upon minimizing the Gibbs' free energy of the system. We used the RGIBBS block in ASPEN Plus to perform the chemical equilibrium calculations. No experimental data were used in this calculation, and no specific chemical reactions were entered. Thus, comparing the model predictions with these earlier ASPEN calculations will assess whether the model includes enough information about the gas-phase reactions. Figure 7 shows that the model predictions agree extremely well with the thermodynamic chemical equilibrium calculations for lignin at the base case conditions (600°C). In both cases, H_2 and CO_2 are the major products (35–45% each), with about 25% of CH_4 and a very small mole % of CO.

It is important to make a note here about the water–gas shift reaction in SCW. Under more conventional gasification conditions, the water–gas shift reaction at this temperature would produce a much higher mole fraction of CO at equilibrium. In SCW, however, equilibrium is shifted strongly in the direction of CO consumption. Thus, SCWG could be very useful for making H_2 with a very low CO content (e.g., for use in PEM fuel cells).

This section showed that the kinetics model can predict the outcomes of experiments for a range of biomass loadings and water densities, and that equilibrium predictions also agree with thermodynamic calculations. Additionally, Resende[23] showed that the model predictions for the effects of biomass loading and water density on the equilibrium compositions agreed reasonably well with the results from Gibbs free energy minimization. These successes indicate that the reactions included in the model and the parameter estimates are adequate for describing the noncatalytic SCWG of lignin and cellulose under the conditions explored herein.

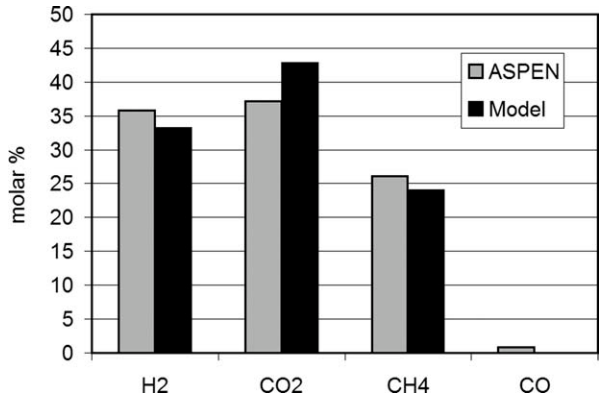

Figure 7. Equilibrium composition for lignin, base case.

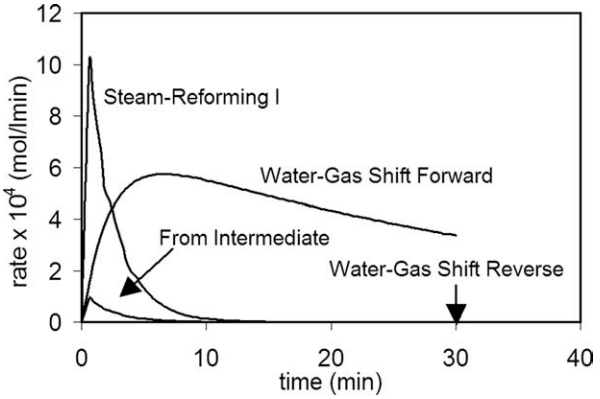

Figure 8. Rates of formation/consumption for H_2 (cellulose, 500°C, 9.0 wt % loading, 0.08 g/ml).

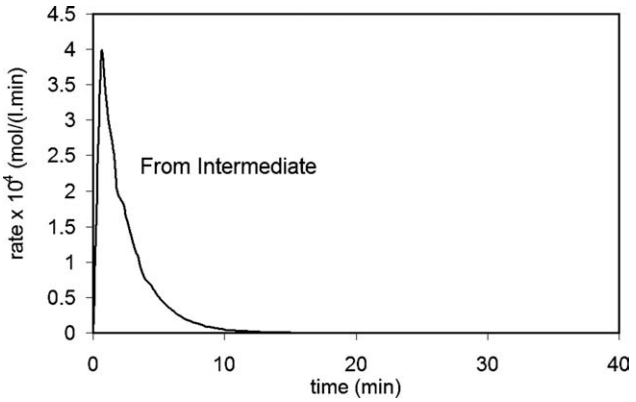

Figure 9. Rates of formation/consumption for CH_4 (cellulose, 500°C, 9.0 wt % loading, 0.08 g/ml).

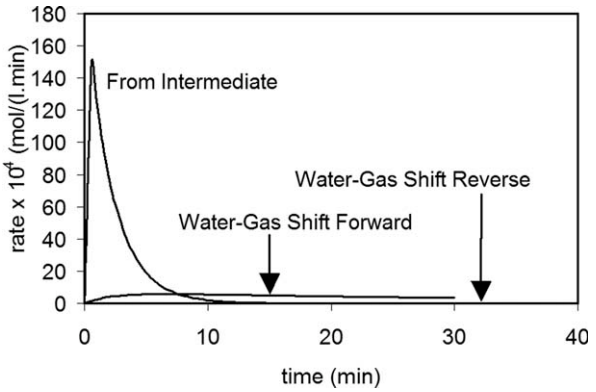

Figure 11. Rates of formation/consumption for CO_2 (cellulose, 500°C, 9.0 wt % loading, 0.08 g/ml).

Reaction rate analysis

The previous sections showed that the model could faithfully reproduce the data used to determine its parameters and that it could predict gas yields and compositions at SCWG conditions not used in the parameter estimation. We now use the model to identify the individual reactions most responsible for the formation and consumption of each gas species during the course of noncatalytic SCWG. More specifically, we calculated the rate of each reaction in the model and then compared the rates for all reactions that produce or consume a specific gaseous product. We show results (Fig. 8–12) for all four gases for cellulose SCWG, but only for H_2 for lignin SCWG. The reactions with the highest rates for CO, CO_2, and CH_4 production were the same for both lignin and cellulose.

Inspection of Figures 8–12 reveal that SCWG at the base case conditions can be viewed as occurring in two distinct temporal regions. At short times (the first few minutes), the gas formation rates reach their highest values. Beyond the first few minutes, the gas production rate is always lower, and the dominant reactions are ones that primarily change the product distribution. For H_2, the high rates of formation in the first minutes are because of steam reforming. Steam reforming I (forming CO) dominates for cellulose, whereas steam reforming II (forming CO_2) dominates for lignin. In both cases, the rate of steam reforming quickly decreases after a few minutes, and the forward rate of the water–gas shift reaction becomes the fastest producer of H_2 at longer periods of time. After reaching a maximum at about 7–8 minutes, the rate of water–gas shift slowly decreases with time. The model results show that the other gas species originate primarily from the collection of lumped intermediates. Direct formation of CH_4 from the intermediate is the most important reaction for CH_4 formation. It appears that a catalyst would be required for the rate of methanation to proceed at a competitive rate. The lumped intermediates are also the main source of CO. Smaller contributions arise from steam-reforming I. The model also indicates that the water–gas shift reaction consumes CO at longer times. The CO_2 originates from intermediates during the first few minutes, but it can also be formed at much smaller rates from water–gas shift at longer times. A key result from this reaction rate analysis is the importance of gas-forming reactions from the numerous intermediate compounds.

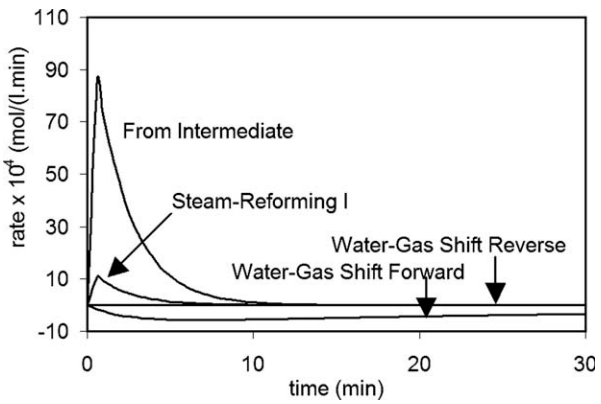

Figure 10. Rates of formation/consumption for CO (cellulose, 500°C, 9.0 wt % loading, 0.08 g/ml).

Sensitivity analysis

A second tool to examine the relative importance of different reaction paths is sensitivity analysis. It reveals how

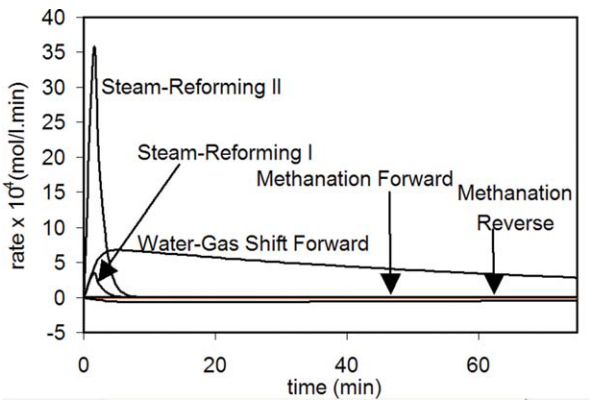

Figure 12. Rates of formation/consumption for H_2 (lignin, 600°C, 9.0 wt % loading, 0.08 g/ml).

[Color figure can be viewed in the online issue, which is available at wileyonlinelibrary.com.]

Table 2. Sensitivity Coefficients for Cellulose SCWG at Base Case Conditions

	CO		CO_2		CH_4		H_2	
Reaction	1 min	30 min	1 min	30 min	1 min	30 min	1 min	30 min
Intermediate Formation	0.225	–	0.230	–	0.228	–	0.255	–
Steam-Reforming I	0.177	–	–	–	–	–	0.979	0.214
Steam-Reforming II	–	–	–	–	–	–	–	–
CO from Intermediate	0.887	0.873	–	0.216	–	–	–	0.669
CO_2 from Intermediate	–	–	0.993	0.753	–	–	–	–
CH_4 from Intermediate	–	–	–	–	1.000	1.023	–	–
H_2 from Intermediate	–	–	–	–	–	–	–	–
Char Formation	−0.131	−1.008	−0.129	−0.931	−0.130	−0.921	−0.119	−0.944
Water-gas Shift	–	−0.678	–	0.166	–	–	–	0.553
Methanation	–	–	–	–	–	–	–	–

the predictions of a model (concentration of species i (C_i) in this case) change when the value of a single model parameter (rate constants (k_j) in this case) is slightly perturbed. The normalized sensitivity coefficient, S_{ij}, captures this influence of the parameter k_j on the outcome, and it can be defined as in Eq. 11:

$$S_{i,j} = \frac{\partial \ln C_i}{\partial \ln k_j} = \frac{\Delta C_i / C_j}{\Delta k_j / k_j} \tag{11}$$

We calculated the sensitivity coefficients manually by perturbing each rate constant by 5% one at a time, running the kinetics model, and recording ΔC_i for each gaseous product for each case. The reaction rate analysis showed that different reactions dominate noncatalytic SCWG at short times and at longer times. Therefore, we examined the sensitivities at both short times (1 min) and long times (30 min for cellulose and 75 minutes for lignin). Tables 2 and 3 show the results and only sensitivity coefficients with an absolute value exceeding 0.1 are included. These reactions are the ones in which the relative change in gas concentration was at least 10% as large as the relative change in the rate constant.

At 1 min, the concentrations of CO, CO_2, and CH_4 from both lignin and cellulose are most sensitive to the rate of formation of these gases from the many lumped intermediate compounds. The sensitivity coefficients are nearly equal to unity. Their positive value means that increasing the rate constant for one of these reactions will increase the calculated gas concentration. This result is an important one because it indicates that the hydrothermal reactions of intermediate compounds are very important for producing gases via noncatalytic SCWG. The concentration of H_2 at 1 min from both lignin and cellulose was most sensitive to the rate constants for steam reforming.

At long times, the concentrations of CO, CO_2, and CH_4 still displayed strong sensitivity to the rate constants for their formation from intermediates, but there was often an even stronger sensitivity to the rate constant for the reaction wherein intermediates formed char. Likewise, the H_2 concentration at long times showed a large sensitivity to the rate constant for char formation, but it was also sensitive to the water–gas shift kinetics and the rate constant for CO formation from intermediates. Of course, CO is a reactant in the water–gas shift reaction, so these latter two sensitivities are related. A key result from this sensitivity analysis at long times is that the competition between char formation and gas formation has a profound influence on the gas yields from noncatalytic SCWG of lignin and cellulose. Again we see the hydrothermal reactions of the species lumped together as intermediates in this model being central to the determination of gas yields and compositions.

Conclusions

(1) This article presents the first quantitative kinetics model for gas production from noncatalytic SCWG of biomass components. The set of 11 reactions and the concept of a generic reactive intermediate proved sufficient for fitting the base case experimental data for the cellulose and lignin samples investigated and predicting gas concentrations at different biomass loadings and water densities. The model's equilibrium predictions agree with

Table 3. Sensitivity Coefficients for Lignin SCWG at Base Case Conditions

	CO		CO_2		CH_4		H_2	
Reaction	1 min	75 min	1 min	75 min	1 min	75 min	1 min	75 min
Intermediate Formation	0.496	–	0.501	–	0.499	–	0.503	–
Steam-Reforming I	–	–	–	–	–	–	–	–
Steam-Reforming II	–	–	–	–	–	–	0.864	0.373
CO from Intermediate	0.963	0.930	–	0.247	–	–	–	0.355
CO_2 from Intermediate	–	–	0.868	0.646	–	–	–	–
CH_4 from Intermediate	–	–	–	–	0.999	0.966	–	–
H_2 from Intermediate	–	–	–	–	–	–	–	–
Char Formation	−0.635	−0.884	−0.637	−0.930	–	−0.966	−0.637	−0.760
Water-gas Shift	–	−0.844	–	0.160	–	–	–	0.410
Methanation	–	–	–	–	–	–	–	−0.179

thermodynamic calculations, and the rate constants obtained for the water–gas shift reaction are in the same range as values reported from careful investigations of this reaction in supercritical water. This modeling framework may be useful for SCWG of other biomass materials and for catalyzed SCWG systems.

(2) The model showed that the identities of the fastest SCWG reaction paths differ at short times and at longer times. Paths responsible for gas formation from intermediates are most important at short times, whereas paths that redistribute the different gases (e.g., water gas shift) become most important at longer times.

(3) H_2 is mostly formed via steam-reforming at short times and from water–gas shift at longer times. CO, CO_2 and CH_4, on the other hand, form predominantly via hydrothermal reactions of the many intermediate species. Steam reforming is not the major contributor to either CO or CO_2.

(4) The model results show clearly that the reactions of intermediates, compounds smaller than the biomass monomer but larger than the C_1 gases, largely determine the outcome of noncatalytic SCWG. Therefore, improved knowledge about the reactions of small organic compounds under SCWG conditions could lead to an improved understanding of the key aspects of the operative chemistry.

Acknowledgments

F. L. P. R. gratefully acknowledges the Ph.D. fellowship awarded from the CNPq, an institution of the Brazilian Government committed to promote research and higher education. This research was also supported by the National Science Foundation (CBET-0755617).

Literature Cited

1. Matsumura Y, Sasaki M, Okuda K, Takami S, Ohara S, Umetsu M, Adschiri T. Cellulose hydrolysis in subcritical and supercritical water. *Comb Sci Technol*. 2006;178:509–536.
2. Boukis N, Diem V, Habicht W, Dinjus E. Methanol reforming in supercritical water. *Ind Eng Chem Res*. 2003;42:728–735.
3. Antal MJ, Allen SG, Schulman D, Xu X, Divilio RJ. Biomass gasification in supercritical water. *Ind Eng Chem Res*. 2000;39:4040–4053.
4. Osada M, Sato O, Watanabe M, Arai K, Shirai M. Water density effect on lignin gasification over supported noble metal catalysts in supercritical water. *Energy Fuels*. 2006;20:930–935.
5. Schmieder H, Abeln J, Boukis N, Dinjus E, Kruse A, Kluth M, Petrich G, Sadri E, Schacht. Hydrothermal gasification of biomass and organic wastes. *J Supercritical Fluids*. 2000;17:145–153.
6. Elliott DC. Catalytic hydrothermal gasification of biomass. *Biofuels Bioprod Bioref*. 2008;2:254–265.
7. Yoshida Y, Dowaki K, Matsumura Y, Matsuhashi R, Li D, Ishitani H, Komiyama H. Comprehensive comparison of efficiency and CO_2 emissions between biomass energy conversion technologies-position of supercritical water gasification in biomass technologies. *Biomass Bioenergy*. 2003;25:257–272.
8. Lee I, Kim M, Ihm S. Gasification of glucose in supercritical water. *Ind Eng Chem Rev*. 2002;41:1182–1188.
9. McHugh MA, Krukonis VJ. Supercritical fluid extraction: principles and practice. Supercritical Fluid Extraction. 1986, 512.
10. Martino CJ, Savage PE, Kasiborski J. Kinetics and products from o-Cresol oxidation in supercritical water. *Ind Eng Chem Res*. 1995; 34:1941–1951.
11. Matsumura Y, Minowa T, Potic B, Kersten SRA, Prins W, van Swaaij WPM, van de Beld B, Elliott DC, Neuenschwander GG, Kruse A, Antal MJ. Biomass gasification in near- and supercritical water: status and prospects. *Biomass Bioenergy*. 2005;29:269–292.
12. Fang Z, Minowa T, Smith RL, Ogi T, Kozinski JA. Liquefaction and gasification of cellulose with Na2CO3 and Ni in subcritical water at 350°C. *Ind Eng Chem Res*. 2004;43:2454–2463.
13. Kruse A, Henningsen T, Sinag A, Pfeiffer J. Biomass gasification in supercritical water: influence of the dry matter content and the formation of phenols. *Ind Eng Chem Res*. 2003;42:3711–3717.
14. Herguido J, Corella J, Gonzalez-Saiz J. Steam gasification of lignocellulosic residues in a fluidized bed at a small pilot scale. Effect of the type of feedstock. *Ind Eng Chem Res*. 1992;31:1274–1282.
15. Kabyemela BM, Adshiri T, Malaluan RM, Arai K. Kinetics of glucose epimerization and decomposition in subcritical and supercritical water. *Ind Eng Chem Res*. 1997;36:1552–1558.
16. Schwald W, Bobleter O. Hydrothermolysis of cellulose under static and dynamic conditions at high temperatures. *J Carbohydr Chem*. 1989;8:565–578.
17. Matsumura Y. Biomass gasification in near- and supercritical water: Status and prospects. *Energ Convers Manag*. 2002;43:1301–1310.
18. D'Jesus P, Boukis N, Kraushaar-Czarnetzki B, Dinjus E. Influence of process variables on gasification of corn silage in supercritical water. *Ind Eng Chem Res*. 2006;45:1622–1630.
19. Resende FLP, Savage PE. Expanded and updated results for supercritical water gasification of cellulose and lignin in the absence of metals. *Energy Fuels*. 2009;23:6213–6221.
20. Resende FLP, Fraley SA, Berger MJ, Savage PE. Noncatalytic gasification of lignin in supercritical water. *Energy Fuels*. 2008;22: 1328–1334.
21. Sasaki M, Kabyemela B, Malaluan R, Hirose S, Takeda N, Adschiri T, Arai K. Cellulose hydrolysis in subcritical and supercritical water. *J Supercritical Fluid*. 1998;13:261–268.
22. Bobleter O. Hydrothermal degradation of polymers derived from plants. *Progress Polym Sci*. 1994;19:797–841.
23. Resende FLP. Supercritical Water Gasification of Biomass. PhD Thesis. University of Michigan, Ann Arbor, MI, 2009.
24. Simmons GM, Gentry M. Particle size limitations due to heat transfer in determining pyrolysis kinetics of biomass. *J Anal Appl Pyrolysis*. 1986;10:117–127.
25. Vamvuka E, Karakas E, Kastanaki E, Grammelis P. Pyrolysis characteristics and kinetics of biomass residuals mixtures with lignite. *Fuel*. 2003;82:1949–1960.
26. Rice SF, Steeper RR, Aiken JD. Water density effects on homogeneous water-gas shift reaction kinetics. *J Phys Chem A*. 1998;102: 2673–2678.
27. Araki K, Fujiwara H, Sugimoto K, Oshima Y, Koda S. Kinetics of water-gas shift reaction in supercritical water. *J Chem Eng Jpn*. 2004;37:443–448.
28. Sato T, Kurosawa S, Smith RL, Adschiri T, Arai K. Water gas shift reaction kinetics under noncatalytic conditions in supercritical water. *J Supercritical Fluids*. 2004;29:113–119.

Manuscript received Aug. 1, 2009, and revision received Nov. 7, 2009.